INSTITUTE OF PHYSICS PUBLISHING PHYSIOLOGICAL MEASUREMENT

Physiol. Meas. **23** (2002) 385–401 PII: S0967-3334(02)27770-9

Relationship between detrended fluctuation analysis and spectral analysis of heart-rate variability

Keith Willson[1], Darrel P Francis[1,2], Roland Wensel[2], Andrew J S Coats[1,2] and Kim H Parker[3]

[1] Department of Biomedical Engineering, Royal Brompton Hospital, Sydney St., London SW3 6NP, UK
[2] National Heart and Lung Institute, Dovehouse St., London SW3 6LY, UK
[3] Department of Bioengineering, Imperial College of Science, Technology and Medicine, Exhibition Road, London SW7 2AZ, UK

E-mail: k.willson@rbh.nthames.nhs.uk

Received 10 August 2001, in final form 2 November 2001
Published 21 March 2002
Online at stacks.iop.org/PM/23/385

Abstract

The recently-introduced technique of detrended fluctuation analysis (DFA) for heart-rate variability appears to yield improved prognostic power in cardiovascular disease through calculation of the fractal scaling exponent α. However, the physiological meaning of α remains unclear. In DFA, the signal is segmented into lengths from 4 to 64 beats. For each segmentation length (n), the individual segments are cumulated, detrended and the sum of the squares (F^2) of residuals calculated. α is the slope of $\log(F)$ against $\log(n)$. We show mathematical equivalence between α calculated by DFA and by a novel alternative method using frequency-weighted power spectra.

We show F^2 (and thus α) can be obtained from a frequency-weighted power spectrum without DFA. To do this, we cumulate and detrend the Taylor series of individual Fourier components. F^2 is found to depend on the relationship between the signal period and segment length. F^2 can therefore be expressed in terms of frequency-weighted power spectra. From this, the α coefficient of DFA can then be described in power-spectral terms, which facilitates exploration of its physiological basis. We confirm these findings using samples from 20 healthy volunteers and 40 patients with heart failure.

Keywords: heart-rate variability, fractal scaling, detrended fluctuation analysis, spectral analysis, periodic breathing, heart failure

Nomenclature

A	amplitude of Fourier component of signal
D	residual after cumulation and detrending
F^2	mean of squares of residuals
N	length of data set in samples
$P(f)$	power spectrum of the signal
R	coefficient combining all the coefficients of Δ^u
a,b	slope and intercept of least-squares regression line
f	frequency of signal component, in cycles per second
f_s[4]	the sampling frequency, in samples per second
k	constant of integration
n	length of analysis segment in samples
p	integer indexing terms within Taylor series expansion
u	integer indexing terms within series expansion of squared residual
r_p	fraction of the pth term of the Taylor series expansion of a single frequency component remaining after cumulation and detrending
Δ	length of analysis segment, in radians at the frequency of the signal component ($=\omega n$)
α	slope of log–log plot of F and n
δ	sample distance from the central sample in an analysis segment
τ	sample number
ω	angular frequency of signal component, in radians per second ($=2\pi f$)
ω_s	angular frequency of sampling, in radians per second ($=2\pi f_s$)

1. Introduction

Measurement of heart-rate variability (HRV) is a technique of growing importance for assessing risk in patients with cardiovascular disease. Extensive experience has been accumulated regarding the diagnostic and prognostic value of spectral analysis to quantify components of heart-rate variability (Pagani *et al* 1986, Malliani *et al* 1991, Task Force 1996, La Rovere *et al* 1997, 1998). Conventional spectral analysis protocols based on Fourier or autoregressive spectral estimates recognize distinct standardized frequency ranges. Specifically, these are the respiratory ('high frequency', HF) band from 0.15 to 0.45 Hz, the blood-pressure-mediated ('low frequency', LF) band from 0.05 to 0.15 Hz and the 'very low frequency' (VLF) band which may arise by several mechanisms including periodic breathing (Mortara *et al* 1997, Francis *et al* 2000) that occurs in some patients with chronic heart failure.

Recently, a new approach to heart-rate variability, detrended fluctuation analysis (DFA), has been introduced, arising from fractal analytical techniques (Peng *et al* 1995, Ho *et al* 1997). In this approach, values α_1 and α_2 (said to be fractal scaling exponents) are calculated using a short-term frequency range (4–16 heart beats for α_1) and a longer range (16–64 heartbeats for α_2). These measures, particularly α_1, have been found to have prognostic power for patients with chronic heart failure (Ho *et al* 1997). Further work has suggested that measurement of α_1 may give greater prognostic power than assessment of conventional spectral measures (Huikuri *et al* 2000, Pikkujamsa *et al* 1999, Perkiomaki *et al* 2001).

[4] In this analysis we index the elements of the data series by sample number, which allows maximum generality, since it does not limit the interpretation to RR interval series. If a slightly simpler format, restricted to RR interval series, is required, f_s can be taken as 1 and the data series is then addressed by beat number (=sample number).

This DFA approach to heart-rate variability analysis suffers from uncertainty about the meaning of the α coefficients that are obtained. A great deal is known about how physiological processes influence heart rate and thus generate spectral components in heart-rate variability, but it is unclear precisely which aspects of this physiology affect the DFA indices. Without such understanding there is no guidance for interpreting the observed empirical relations between certain values seen on DFA and higher mortality.

We develop an analysis of the α values for DFA in terms of conventional spectral measures whose relationship to physiology is widely recognized and well validated. A series of mathematical steps is presented which shows the close link between these DFA α values (said to be fractal measures) and conventional power-spectral ratios. We then verify this analysis by determining the agreement between DFA α values and modified power-spectral measures, using physiological data. Ultimately this mathematical analysis will enable us to explain what the DFA indices mean in physiological terms and to speculate rationally on why they may show prognostic value in patients with cardiac disease.

1.1. Detrended fluctuation analysis

Detrended fluctuation analysis is a procedure which generates α, which is presented in the clinical literature as a measure of fractal scaling behaviour. This assumption arises from the steps involved in DFA, which evaluate how the amplitude of fluctuations in a signal depends on the scale over which they are measured.

For DFA, the R–R interval sequence is divided into equal, non-overlapping segments. In each segment, the data are first cumulated, and then detrended by subtraction of the least squares linear regression line. The squares of the cumulated, detrended data points (residuals) are then averaged over the whole data set and the square root of the mean residual found. This gives a value of the fluctuation (F) of the time series for the given segment length.

This operation is performed for divisions of the data into segment lengths of between 4 and 400 data points. The α value is obtained as the slope of the linear regression line through a log–log plot of the sums of the squares of the residuals against the segment length, between defined values of segment length. For example, α_1 is calculated over the range of segment lengths between 4 and 16 data points.

2. Analysis of detrended fluctuation analysis in Fourier terms

We aim to obtain F^2 (and therefore α) in terms of the power spectrum of the signal. We start with a single harmonic component of the signal, and examine the effect of cumulation and detrending on a Taylor series expansion for differing segmentation lengths. We show how the squared residuals depend upon segment length, and how this differs according to whether the signal period is shorter or longer than the segment length. We then show, for any segment length, how the combination of the squared residual terms (i.e. F^2) can be expressed as a frequency-weighted power spectrum. This yields α without DFA.

Finally, we observe that an approximate analytical expression for α can be obtained from the analytical expression for F^2.

We start by expressing the chain of operations on the signal used for the DFA mathematically, for a single harmonic component of the signal.

2.1. Behaviour of single harmonic component on detrended fluctuation analysis

Consider a single harmonic (Fourier) component of a time series:

$$S(t) = A\cos(\omega t).$$

(We present the argument here for a cosine component; a similar process is valid for sine functions, hence the argument may be extended to signals of arbitrary phase.)

2.2. Cumulation

The integrated function $I(\tau)$, over a data segment from time τ_0 to τ, is

$$I(\tau) = \int_{t=\tau_0}^{t=\tau} S(t)\,\mathrm{d}t = (A/\omega)\sin(\omega\tau) + k \tag{1}$$

where $k = -(A/\omega)\sin(\omega\tau_0)$.

Cumulation of discrete time series is a similar process, but introduces a factor of ω_s which is $2\pi f_s$, where f_s is the sampling frequency. This is because higher sampling rates result in greater cumulative totals.

$$C(\tau) = \omega_s I(\tau) = A\frac{\omega_s}{\omega}\sin(\omega\tau + \delta) + \omega_s k.$$

2.3. Detrending

The Taylor series expansion for the function $C(\tau + \delta)$ about a particular value of $\omega\tau$, is given by:

$$C(\tau+\delta) = A\frac{\omega_s}{\omega}\sum_{p=0}^{\infty}\begin{pmatrix}(-1)^{\frac{p}{2}}\frac{\delta^p}{p!}\sin(\omega\tau) & \text{for even } p\\ (-1)^{\frac{p-1}{2}}\frac{\delta^p}{p!}\cos(\omega\tau) & \text{for odd } p\end{pmatrix} + \omega_s k \tag{2}$$

where p is an integer. To detrend $C(\tau + \delta)$, its least squares regression line is subtracted:

$$D(\tau+\delta) = C(\tau+\delta) - a(\tau+\delta) - b. \tag{3}$$

This process removes both the mean value (b) and a linear slope (a).

Linear detrending of $C(\tau)$ removes the $\sin(\omega\tau) + \delta\cos(\omega\tau)$ terms, together with additional constant and linear contributions arising from the higher order terms in δ. The odd terms in (2) contribute to the linear component $a(\tau + \delta)$ in equation (3), while the even terms contribute to the constant b in equation (3). Also removed is the constant of integration, corresponding to k in equation (1). Linear detrending is therefore equivalent to multiplying each term in the Taylor series expansion by an associated factor r. Hence the signal in the cumulated and detrended segment becomes

$$D(\tau+\delta) = A\frac{\omega_s}{\omega}\sum_{p=0}^{\infty}\begin{pmatrix}r_p(-1)^{\frac{p}{2}}\frac{\delta^p}{p!}\sin(\omega\tau) & \text{for even } p\\ r_p(-1)^{\frac{p-1}{2}}\frac{\delta^p}{p!}\cos(\omega\tau) & \text{for odd } p\end{pmatrix} \tag{4}$$

where $r_p = \frac{p}{p+1}$ for p even; $r_p = \frac{p-1}{p+2}$ for p odd.

The factor r_p is derived by comparing the mean of the integral of the product of δ^p over the region $-\delta/2$ to $+\delta/2$ with that of the mean of the integral of the product of the detrended functions over the same region. They are different for odd and even values of p because detrending is equivalent to simply removing the mean from even-powered terms in δ and a linear slope from odd-powered terms in δ.

2.4. Mean-squared residuals

Squaring the expression in equation (4) gives the squared residuals:

$$D^2(\tau+\delta) = \left(A\frac{\omega_s}{\omega}\right)^2 \times \begin{pmatrix} \sin^2(\omega\tau)\sum_{p_1=0}^{\infty}\sum_{p_2=0}^{\infty}(-1)^{\frac{p_1+p_2}{2}-1}\frac{p_1p_2}{(p_1+1)(p_2+1)}\frac{\delta^{p_1+p_2}}{p_1!p_2!} & \text{for } p_1,\ p_2 \text{ even} \\ +\cos^2(\omega\tau)\sum_{p_1=1}^{\infty}\sum_{p_2=1}^{\infty}(-1)^{\frac{p_1+p_2}{2}}\frac{(p_1-1)(p_2-1)}{(p_1+2)(p_2+2)}\frac{\delta^{p_1+p_2}}{p_1!p_2!} & \text{for } p_1,\ p_2 \text{ odd} \\ +\sin(\omega\tau)\cos(\omega\tau)\sum_{p_1=0}^{\infty}\sum_{p_2=1}^{\infty}(-1)^{\frac{p_1+p_2-1}{2}}\frac{p_1(p_2-1)}{(p_1+1)(p_2+2)}\frac{\delta^{\frac{p_1+p_2-1}{2}}}{p_1!p_2!} & \text{for } p_1 \text{ even},\ p_2 \text{ odd} \\ +\sin(\omega\tau)\cos(\omega\tau)\sum_{p_1=1}^{\infty}\sum_{p_2=0}^{\infty}(-1)^{\frac{p_1+p_2-1}{2}}\frac{(p_1-1)p_2}{(p_1+2)(p_2+1)}\frac{\delta^{\frac{p_1+p_2-1}{2}}}{p_1!p_2!} & \text{for } p_1 \text{ odd},\ p_2 \text{ even} \end{pmatrix}. \tag{5}$$

A segment of length n samples covers a phase angle of Δ radians, where $\Delta = n\omega$. This is from sample number $\omega\{\tau - n/2\}$ to $\omega\{\tau + n/2\}$. The mean-square residual over this segment is

$$\overline{D^2} = \frac{1}{\Delta}\int_{\delta=-\frac{\Delta}{2}}^{\delta=\frac{\Delta}{2}} D^2(\tau+\delta)\,\mathrm{d}\delta.$$

Integrating with respect to δ is equivalent to summing terms of the following form, where $u = p_1+p_2$ and R_u is a coefficient combining all the coefficients of δ^u arising from equation (5):

$$\frac{R_u}{\Delta}\int_{\delta=-\frac{\Delta}{2}}^{\delta=\frac{\Delta}{2}} \delta^u\,\mathrm{d}\delta.$$

The integration yields $\frac{R_u\Delta^u}{2^u(u+1)}$. Taking the mean-square residual over the whole data set is equivalent to multiplying each power term in Δ, considered constant, by the mean of its associated oscillatory term.

The oscillatory terms $\sin^2(\omega\tau)$, $\sin(\omega\tau)\cos(\omega\tau)$ and $\cos^2(\omega\tau)$ oscillate at twice the frequency of $\sin(\omega\tau)$. The odd values of u are associated with the $\sin(\omega\tau)\cos(\omega\tau)$ oscillatory terms whose means tend to 0 when averaged over the whole data set, and therefore for odd u, the $\frac{R_u\Delta^u}{2^u(u+1)}$ term can be neglected.

The even values of u are associated with the $\sin^2(\omega\tau)$ and $\cos^2(\omega\tau)$ oscillatory terms which tend to $\frac{1}{2}$ over the whole data set, irrespective of the value of ω, provided that the data set contains at least half a period of the component in $\omega\tau$. Hence

$$\overline{D^2} \approx \frac{1}{2}\left(A\frac{\omega_s}{\omega}\right)^2 \sum_{u=0}^{\infty}\begin{pmatrix} \frac{R_u\Delta^u}{2^u(u+1)} & \text{for even } u \\ 0 & \text{for odd } u \end{pmatrix}.$$

It is useful to observe that since only the even values of u are relevant, and the mean and linear trends are removed (corresponding to $u = 0$ and 2 because of squaring), the summing term effectively begins at $u = 4$. Moreover, since $\Delta = n\omega$, this expression is equivalent to

$$\overline{D^2} = \frac{1}{2}\left(A\frac{\omega_s}{\omega}\right)^2 \sum_{u=4}^{\infty}\frac{R_u}{(u+1)}\left(\frac{n\omega}{2}\right)^u \tag{6}$$

with u restricted to even values.

In a segment of length Δ, the behaviour of the residual sum of squares is dependent on whether the segment is longer or shorter than one cycle of the oscillation.

2.5. Residual sum of squares with segment (Δ) shorter than one cycle

If the segment is short in comparison to a cycle, then $n\omega$ is always small, so the residuals after detrending are dominated by the term $(n\omega)^4$ so that equation (6) becomes

$$\overline{D^2} \approx \frac{1}{2}\left(A\frac{\omega_s}{\omega}\right)^2 \frac{R_4}{5}\left(\frac{n\omega}{2}\right)^4.$$

Since from equation (5), R_4 is $\frac{2}{(2+1)}\frac{2}{(2+1)}\frac{1}{2!2!} = \frac{1}{9}$. This allows (6) to be simplified to

$$\overline{D^2} \approx \frac{\omega_s^2 A^2 \omega^2}{1440} n^4. \tag{7}$$

We tested this 4th-power relationship numerically in Matlab™ (figures 1 and 2) in order to demonstrate the effect of the length of the segment window upon the cumulation, detrending and ultimately the mean-squared residual of a Fourier component of the signal. Figure 1 demonstrates the effect of changing the segment length (at constant signal frequency) or signal frequency (at constant segment length) at each stage of the process. When the frequency is halved the mean-squared residual falls by a factor of 4; when the segment length is doubled the mean-squared residual is found to increase by a factor of 16.

2.6. Residual sum of squares with segment (Δ) longer than one cycle

Now consider the residuals when Δ is large, i.e. greater than one cycle. As the number of cycles of the sinusoid in the interval Δ increases, the trend approaches zero. In this case, the residuals, after detrending, approximate to the sinusoid itself. The mean-squared residual is simply the mean-square value of the cumulated sinusoid weighted by a frequency-dependent factor (introduced by the original cumulation process) and by the sampling frequency.

$$\overline{D^2} \approx \frac{1}{2}\left(A\frac{\omega_s}{\omega}\right)^2. \tag{8}$$

2.7. Overall dependence of residual sum of squares on segment length

In figure 2 we show the dependence of the mean-squared residual upon the segment length across a wide range of segment lengths. This confirms, for low n, the predominant fourth-power relationship between $\overline{D^2}$ and n, predicted in equation (7) and shown in the figure by the oblique line. It also confirms, for higher values of n, the independence of $\overline{D^2}$ from segment length, as shown by the horizontal line arising from equation (8). The transition between the two regions would require a large increase in number of terms within the Taylor series without significant increase in fidelity.

2.8. Multiple spectral components

A general signal is a linear combination (with spectrum $P(f)$) of Fourier components whose contribution to $P(f)$ at each frequency is simply A^2. Since they are orthogonal functions the cross-products of the Fourier components are all zero, the overall residual sum of squares of the complete signal (F^2) is equal to the sum of the contributions $\overline{D^2}$ from each Fourier component A^2 as shown in equations (7) and (8).

The nature of the contribution at any frequency depends upon whether its wavelength is shorter or longer than the segment length n, as shown above. Therefore, for any given segment length, n, high-frequency components ($f > 1/n$) contribute from their plateau regions as described by equation (8). Meanwhile low-frequency components ($f < 1/n$) contribute from their quartic region as described by equation (7). Thus, writing in terms of $f = \omega/2\pi$,

$$\begin{aligned} F^2(n) &= \frac{\omega_s^2 n^4}{1440}\int_{1/N}^{1/n}(2\pi f)^2 P(f)\,\mathrm{d}f + \frac{\omega_s^2}{2}\int_{1/n}^{1}\frac{P(f)}{(2\pi f)^2}\,\mathrm{d}f \\ &= \frac{\omega_s^2}{8\pi^2}\left[cn^4\int_{1/N}^{1/n} f^2 P(f)\,\mathrm{d}f + \int_{1/n}^{1}\frac{P(f)}{f^2}\,\mathrm{d}f\right] \end{aligned} \tag{9}$$

where $c = \pi^4/45$.

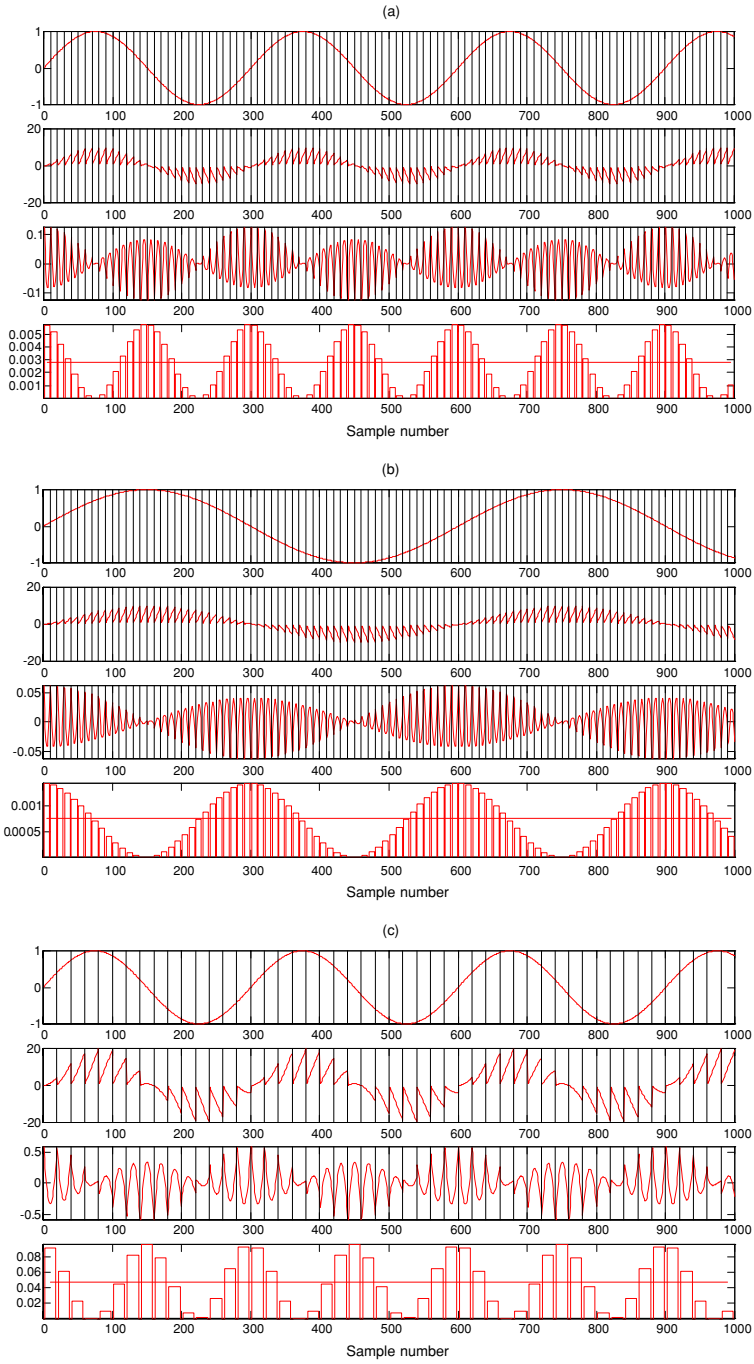

Figure 1. Panel (a) shows a sinusoid of 1000 samples with frequency of 1/300 cycles/sample in segments of $n = 10$. In panel (b) the frequency is changed to 1/600 cycles/sample, while in panel (c) the segment length instead is increased to $n = 20$. In each panel, the first row shows the raw data, the second the effect of cumulation, the third the effect of detrending and the fourth the mean-squared residual in each segment and (superimposed as a horizontal line) the mean-squared residual over the whole data set.

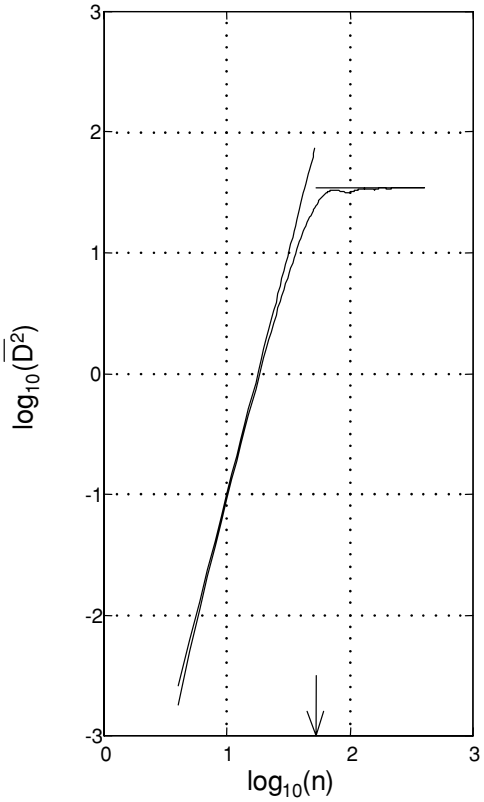

Figure 2. Dependence of $\overline{D^2}$, the mean-squared residual, upon the segment length. A signal consisting of a sinusoid with $\omega = 0.12$ (corresponding to a period of approximately 52 samples) undergoes detrended fluctuation analysis. The mean-squared residual $\overline{D^2}$ is shown as a curve, with the quartic approximation for small n shown as an oblique line and the constant approximation for large n shown as a horizontal line. The value of n corresponding to the period of oscillation of the signal is marked with an arrow.

2.9. Calculation of alpha

The fractal correlation value α is given by the slope of log F against log n. In classical DFA, α is measured over a range of n, but by generalization α can be defined at any n; thus

$$\alpha = \frac{\mathrm{d}[\log_{10} F(n)]}{\mathrm{d}[\log_{10}(n)]}.$$

Using the chain rule

$$\alpha = \frac{1}{2}\frac{\mathrm{d}F^2(n)}{\mathrm{d}n}\frac{n}{F^2(n)}. \tag{10}$$

In order to evaluate (10), we first require an analytical form for $\frac{\mathrm{d}F^2(n)}{\mathrm{d}n}$. We can derive this from our expression for F^2 but must observe the limitations of our single-Taylor-term expansions. As shown in figure 2, our expression gives a good estimate of the slope of F^2 against n, except for in the region of the discontinuity in our piecewise approximation. Thus, when taking the derivative of our expression for F^2,

$$\frac{\mathrm{d}F^2(n)}{\mathrm{d}n} = \frac{\omega_s^2}{8\pi^2}\left[4cn^3\int_{1/N}^{1/n} f^2 P(f)\,\mathrm{d}f - (c-1)P\left(\frac{1}{n}\right)\right]$$

the term $(c-1)P\left(\frac{1}{n}\right)$ arises from this artefactual slope discontinuity and should be disregarded for the purpose of determining α. Thus,

$$\alpha(n, f) = \frac{2}{1 + \frac{\int_{1/n}^{1} \frac{1}{(nf)^2} P(f)\,\mathrm{d}f}{c\int_{1/N}^{1/n} (nf)^2 P(f)\,\mathrm{d}f}}.$$

This shows that the 'fractal correlation coefficient', α, can be expressed in terms of the frequency-weighted power spectrum of the signal.

2.10. Interpreting alpha directly from the frequency-weighted power spectrum

The term $\rho = \frac{\int_{1/n}^{1} \frac{1}{(nf)^2} P(f)\,\mathrm{d}f}{c\int_{1/N}^{1/n} (nf)^2 P(f)\,\mathrm{d}f}$ can be considered to be a modified HF/LF ratio, where the LF part of the spectrum is weighted by in proportion to f^2 and the HF part in proportion to $1/f^2$. The $(nf)^2$ terms result in the weighting being 1 at the junction frequency between the two integrals.

Thus

$$\alpha(f) = \frac{2}{1+\rho}.$$

The value of α becomes <1 when the LF spectrum predominates and >1 when HF predominates. At the extremes, ρ zero and infinity, α becomes 2 and 0, respectively. When $\rho = 1, \alpha = 1$.

The values α_1 and α_2 are obtained as a regression line through the values of α over two distinct ranges of n. For example (Ho *et al* 1997) α_1 has been based on n from 4 to 16 and α_2 on n from 16 to 64. The quantity α_1 can, therefore, simply be considered as a way of expressing a weighted normalized HF/LF ratio and α_2 a weighted normalized LF/VLF ratio.

3. Experimental validation of the spectral approach to α

3.1. Data acquisition

To compare the different approaches to assessing α, we used the data previously obtained for clinical research purposes in 20 healthy volunteers and 40 patients with chronic heart failure. The subjects had been studied in standardized conditions. Each subject had undergone a 10 min recording of heart rate while seated (Francis *et al* 2000). The ECG was acquired from a limb lead, with a well-defined QRS complex, which was usually lead II. In a small number of cases, when a clear R wave was not present in lead II, lead I or lead III was used. The ECG signal was sampled at 1000 Hz using an analogue-to-digital converter (National Instruments, USA) and data acquisition software (Labview®, National Instruments, USA). RR intervals were subsequently determined automatically by custom software in Matlab™ and transients due to ectopy corrected by linear interpolation with previous and following beats.

3.2. Calculation of alpha

To test the hypothesis that F^2 and α can be calculated directly from the power spectrum without DFA, we developed a computer algorithm to implement the steps for standard DFA and for frequency-weighted spectral analysis (equation (9)).

For the frequency-weighted spectral analysis to calculate α, RR intervals were retained at one sample/beat in accordance with standard practice for DFA, and therefore in those power spectra, the unit of frequency is cycles/beat rather than cycles s^{-1} (Hz).

3.2.1. Calculating alpha by standard DFA. Figure 3 (left panel) shows the standard calculation of fractal scaling exponents $\alpha_{1,\mathrm{DFA}}$ and $\alpha_{2,\mathrm{DFA}}$ by DFA. The time-series R–R interval sequence is divided into equal, non-overlapping segments of length n. In each segment, the data are first cumulated and then detrended by subtraction of the least-squares linear regression line. The root-mean-square residual value over the whole data set (F_{DFA}) is then calculated. This operation is performed for divisions of the data into segment lengths (n) of between 4 and 400 data points and the root-mean-square residual F_{DFA} recorded for each n. Then α is calculated as the regression slope of the log–log plot of F_{DFA} against n. Specifically, $\alpha_{1,\mathrm{DFA}}$ is calculated over the range $n = 4$ to $n = 16$ and $\alpha_{2,\mathrm{DFA}}$ between $n = 16$ and $n = 64$.

3.2.2. Calculating alpha by frequency-weighted spectral analysis. We calculated the Fourier spectrum of the data using the (unwindowed) discrete Fourier transform function ('fft') of MATLAB (Mathworks Inc, Natick, MA, USA). We then used equation (9) to yield ${F^2}_{\mathrm{spectral}}$ from which we could obtain values of α (which we denote by $\alpha_{1,\mathrm{spectral}}$ and $\alpha_{2,\mathrm{spectral}}$) as the regression slope of log ${F^2}_{\mathrm{spectral}}(n)$ against log n, using the frequency-weighted power spectrum without the need for DFA (figure 3, right panel).

3.3. Results

The correlation, calculated by the Pearson product-moment method, between the DFA and frequency-weighted spectral methods of measuring α_1 was 0.98 ($p < 0.0001$), with SDD 0.06. For α_2, the correlation between the methods was 0.93 ($p < 0.0001$), with SDD 0.9. Moreover in each case the slope of the regression relationship was 0.99. Figure 4 shows these relationships, with healthy volunteers represented by open circles and patients by filled circles.

4. Discussion

We have now shown how the α obtained from DFA, which has been described as a measure of fractal complexity, can be obtained instead from the power spectrum. Second, we have experimentally observed, in patients and healthy volunteers, a strong agreement between α as measured by the conventional DFA method and as measured by our newly introduced frequency-weighted power-spectral approach. Third, we have drawn an analogy between α and conventional power-spectral ratios. These observations have implications for the physiological and clinical interpretation of α and its prognostic associations, for the concept of α as a unique measure of fractal properties, and for the future development of techniques in heart-rate variability.

4.1. Physiological interpretation of α

Our analysis reveals that the fractal scaling property of heart-rate variability obtained by DFA known as α actually can be obtained via conventional Fourier analysis (equation (9), figure 3) with good concordance (figure 4).

The realization that α_1 and α_2 are related to conventional LF/HF and VLF/LF ratios, respectively enables parallels to be drawn between the apparent fractal properties and physiological processes as conventionally described in power-spectral terms. This opens the way for understanding the physiological meaning of α by its relationship to conventional spectral measures, with their well-established links to physiological processes.

Physiological understanding of heart-rate variability is frequently expressed in terms of the frequency spectrum, specifically the powers in the HF, LF and VLF bands (or the ratios

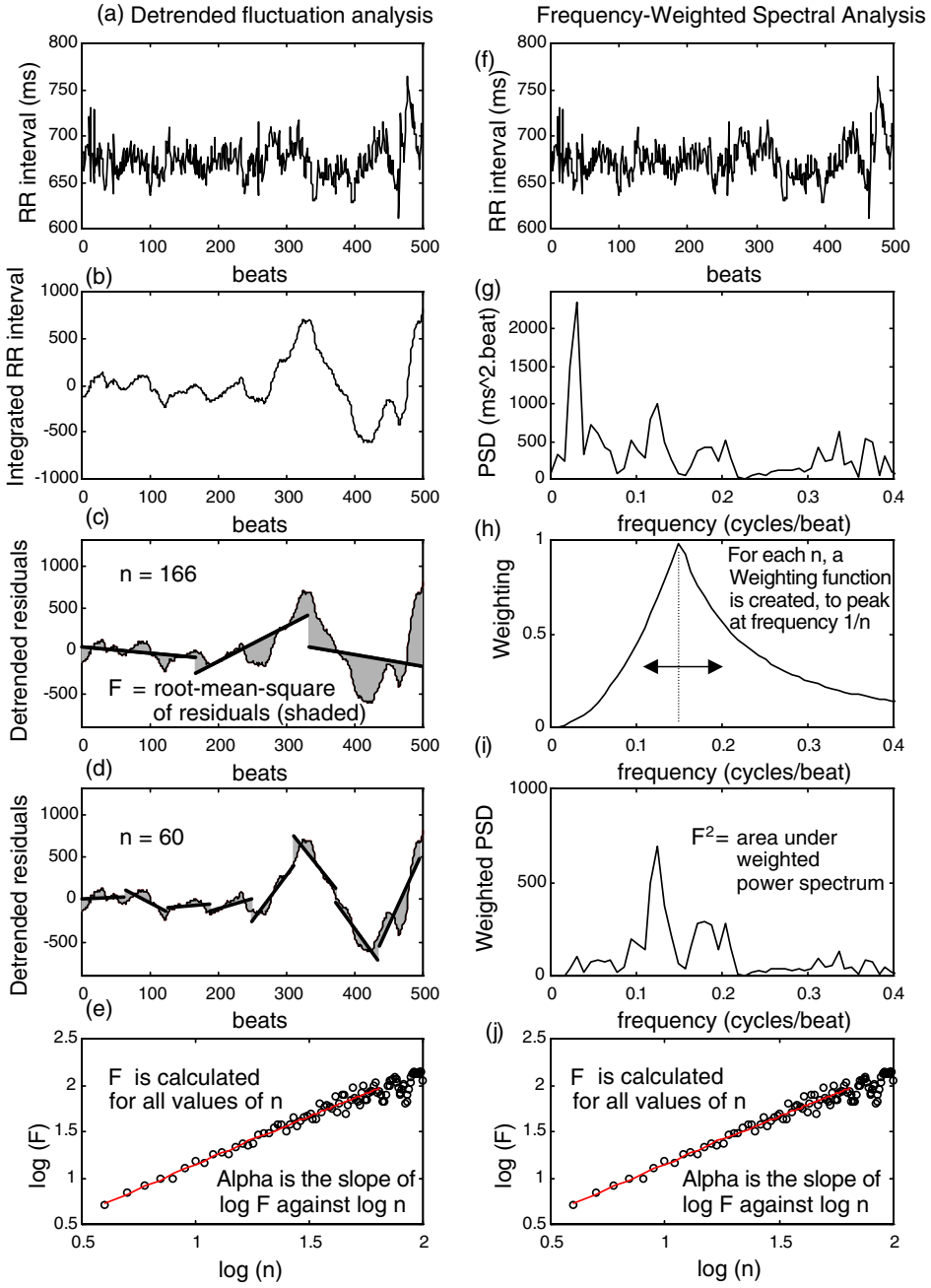

Figure 3. Comparison of calculation of α by DFA and frequency-weighted spectral analysis. In DFA (left) the raw data (a) is cumulated and detrended (b) and then repeatedly approximated by piecewise linear regression with straight segments of length n heartbeats. For each n, F is defined as the root mean square of the residuals (shaded grey). Examples are given for $n = 166$ (c) and $n = 60$ (d). α is the slope of the log–log plot (e) of F against n. The right panels show calculation of α by frequency-weighted power-spectral analysis. The power spectrum (g) is multiplied by the weighting (h), which favours the frequency of interest and decreases proportionally to frequency-squared in both directions. The product, (i), is F^2, from which α is calculated (j) via a $\log(F)$–$\log(n)$ plot.

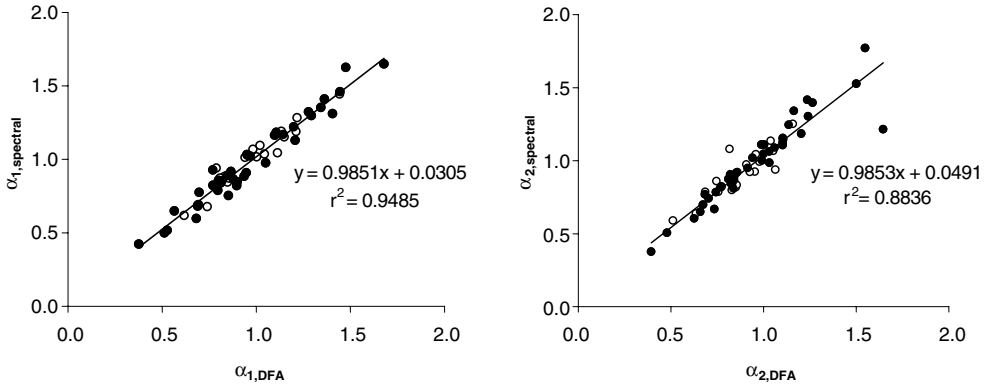

Figure 4. Correlation between methods 1 (DFA) and 2 (frequency-weighted spectral analysis) for α_1 (left panel) and α_2 (right panel). Healthy volunteers ($n = 20$) are represented by open circles and heart failure patients ($n = 40$) by filled circles.

of these powers). The HF/LF spectral ratio has been used for many years in clinical papers as an expression of the 'balance' between sympathetic and vagal activity (Task Force 1996). However, it has been observed that there is little evidence for this interpretation for the HF/LF ratio (Eckberg 1997). The actual neurological mechanisms responsible are likely to be much more complex (Malpas 1998). Notwithstanding this doubt about the precise meaning of this ratio, it is widely quoted and well discussed and forms the basis for many studies in heart-rate variability.

The α values of DFA, which corresponds to frequency-weighted spectral power ratios, differ in several ways (described below).

Nevertheless, there are some similarities between the α values of DFA and conventional power-spectral ratios (figure 5). First, to calculate α_1 the boundary frequency separating weighted L from weighted H ranges from $1/16$ ($\approx$0.06) to $1/4$ (=0.25) cycles/beat. The conventional HF/LF spectral ratio has its boundary at 0.15 cycles s^{-1}. Likewise α_2 has its boundary between $1/64$ ($\approx$0.02) and $1/16$ ($\approx$0.06) cycles/beat, while conventional LF/VLF has its boundary at 0.04 cycles s^{-1}. $\alpha \sim 2\Big/\left(1 + \frac{\text{weighted H}}{\text{weighted L}}\right)$ translates very roughly into unweighted spectral terms as

$$\alpha_1 \sim \frac{2}{1 + \frac{\text{HF power}}{\text{LF power}}} \qquad \alpha_2 \sim \frac{2}{1 + \frac{\text{LF power}}{\text{VLF power}}} \tag{11}$$

4.2. Explanation for prognostic value of α

Early workers on fractal α in chronic heart failure and healthy volunteers displayed on a two-dimensional grid (Ho *et al* 1997) the probability of diagnosis of heart failure given any combination of α_1 and α_2. They observed that normal subjects were clustered at the higher part of the α_1 range and at the lower part of the α_2 range. The other three quadrants (lower α_1 or higher α_2 or both) contained principally patients with chronic heart failure. At that time, no explanation was available for this. We can now offer an explanation in spectral terms. In heart failure, some patients have a decrease in the LF/HF ratio (especially when the disease is advanced), and therefore the $2\Big/\left(1 + \frac{\text{HF}}{\text{LF}}\right)$ ratio may be depressed in these individuals. It is therefore not surprising that α_1 (which resembles the latter) is lower (Lopera *et al* 2001) in

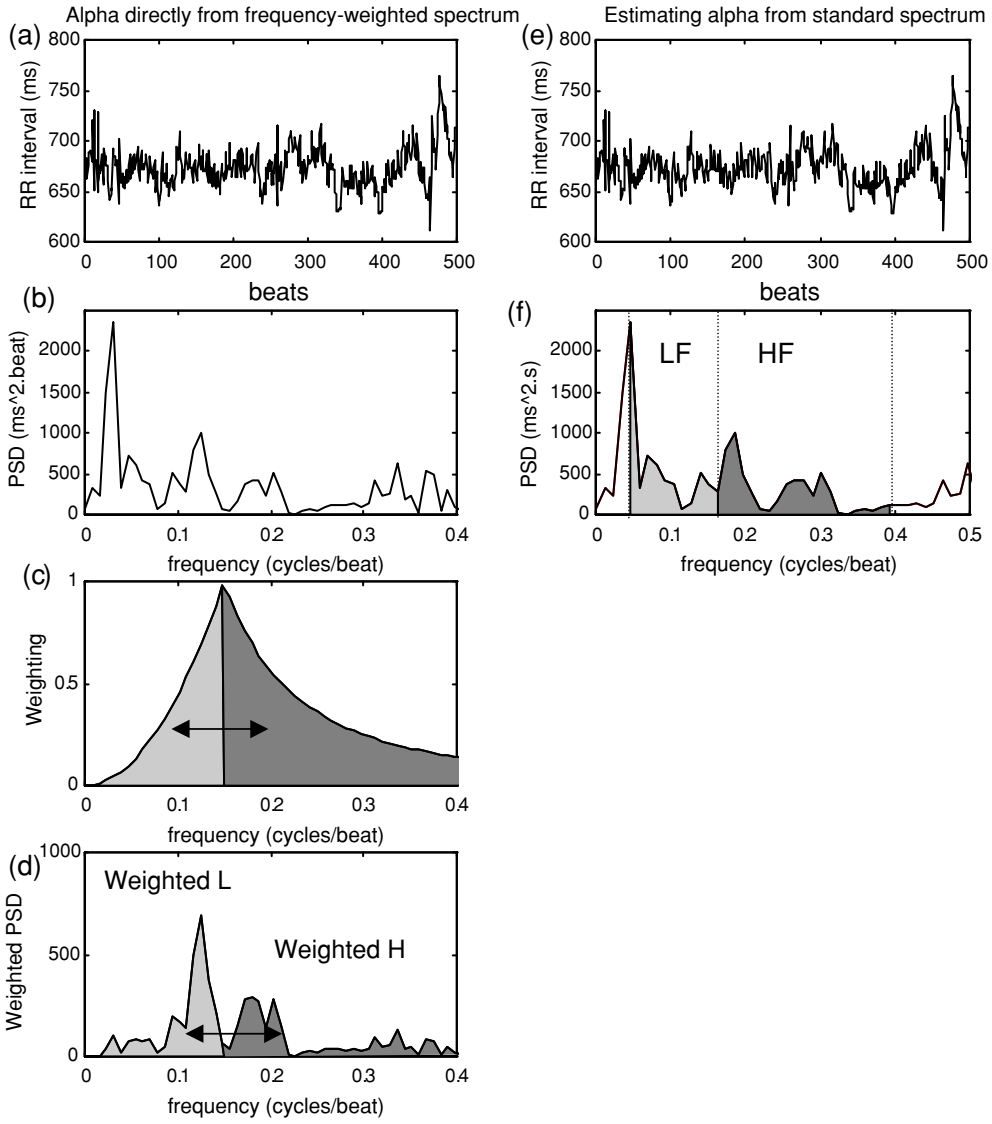

Figure 5. Left panels: from raw data (a), the power spectrum (b) is calculated and multiplied by a 'frequency-weighting' function (c) to yield weighted L and weighted H components (d). α can be estimated as the average value of $2\Big/\left(1+\frac{\text{weighted H}}{\text{weighted L}}\right)$ while the weighting-function's centre frequency is moved through the range of 1/4–1/16 (for α_1) or 1/16–1/64 (for α_2). Right panels: the 'ordinary' power-spectral ratio $2\Big/\left(1+\frac{HF}{LF}\right)$ will behave similarly to α_1, but differs in several details.

patients with severe heart failure than in normals. Heart failure (especially when severe) is also frequently associated with periodic breathing, which can generate corresponding VLF rhythms in heart rate (Mortara *et al* 1997, Francis *et al* 2000). This, alone or in association with the reduced LF, may increase VLF/LF and thus the $2\Big/\left(1+\frac{\text{LF}}{\text{VLF}}\right)$ ratio and α_2.

Since there is a great deal of overlap in the values of α between patients and healthy subjects, the α values are not well suited to distinguishing between these two groups (i.e. diagnosis) especially when the disease is mild and stable (as in our patients). In contrast, other workers have demonstrated that the α values are effective in identifying risk of mortality within a group of subjects who are already diagnosed with heart failure (i.e. prognosis). This distinction, although appearing paradoxical, has been observed by others (Saermark *et al* 2000). Part of the explanation may be the many sources of heart-rate variability that exist. When a patient develops heart failure, the majority of the effects of these influences decrease, but some new phenomena can arise. For example, periodic breathing is known to be able to generate very-low-frequency rhythms in heart rate. Thus VLF rhythms can be an adverse prognostic marker within groups of patients with heart failure, while having no pathological significance when they arise from normal mechanisms in healthy subjects.

4.3. Doubt over α as an independent index of heart-rate variability

We have demonstrated, experimentally, a highly significant association between α and spectral measures and developed a mathematical argument for their equivalence.

We propose, therefore, that α should not be considered a unique cardiovascular indicator in a separate 'fractal' class from conventional power-spectral analysis, because it has a clear and comprehensible grounding in spectral analysis.

The question then arises as to how DFA has been able to provide an apparently improved diagnostic and prognostic role for α when compared with conventional spectral measures. Understanding the differences between these methods allows us to propose a rational mechanism for this prognostic capacity of measurements of fractal complexity.

4.4. Differences between α and conventional spectral analysis

Hitherto published measurement of α standardizes oscillation periods in heartbeats rather than in seconds as in conventional spectral analysis. The time-based approach, with interpolation and resampling applied to the HRV signal, prior to frequency-domain analysis, has become conventional in spectral analysis. The first presentation of DFA in HRV analysis used beat space, and therefore this approach has become the convention for DFA. *A priori*, it is not obvious which approach is better.

These differing conventions lead to differing sensitivities to changes in mean heart rate. For example, α_1, in all patients, refers to the ratio of powers of oscillations whose periods are longer or shorter than approximately eight heartbeats. In contrast, the conventional LF/HF ratio applies to oscillations in fixed frequency ranges, within which the number of heartbeats per cycle depends upon the mean heart rate. Therefore in tachycardia, α addresses a higher frequency region of the power spectrum, and differences in heart rate between subjects may be enough to generate differences in measured α, even if there is no alteration in the actual modulation of heart rate. Older subjects and patients with diseases may have such an increase in mean heart rate (Kaplan *et al* 1991, Yeragani *et al* 1997, Lotric *et al* 2000, Tsuji *et al* 1996).

Conventional power-spectral ratios give equal weighting to all frequencies within these ranges. In contrast, α strongly favours frequencies close to the centre of the range of interest, with frequencies in the outskirts (in either direction) de-emphasized. For example, α_1 can be conceptualized as the average of the ratio of the shaded areas in figure 5(d) as the cut-off is moved from 4 to 16. By inspection, the logarithmic mid-point of this range is 8. Thus, α is

approximately equal to the ratio of the shaded areas when the cut-off is at eight heartbeats per cycle, and frequencies far from this region are markedly de-emphasized. Thus, for example, even if the heart rate is 72 beats per minute so that $1/8$ cycle per beat equals 0.150 Hz, calculation of α_1 will never precisely coincide with the LF/HF ratio.

4.5. Study limitations

To process our experimental data, we used the simple discrete Fourier transformation (without windowing). Had any of the available alternative and more elaborate techniques (Task Force 1996, Kay and Marple 1981) been applied, the results may have been quantitatively different. Time-domain windowing results in the frequency domain response of the window being convolved with that of the signal in the resultant Fourier domain spectrum. Changing the shape of the time domain window redistributes energy between the main beam and the side lobes of the frequency-domain window function. Autoregressive models, if used, are likely to give spectral estimates that vary from those using Fourier transforms, and are sensitive to the order of the model chosen (Christini *et al* 1995, Lotric *et al* 2000). Moreover, if the signal is nonstationary (as all clinical data are to some extent), then the peaks in the power spectrum will in general be flattened with power moving from the peak frequency to the surrounding frequencies.

In general, the values of α are likely to be unaffected, and correspondence between the weighted spectral ratio and DFA is likely to persist if the alternative technique of spectral analysis maintains the overall distribution of power between regions of the spectrum. However, the precise effect on the individual spectra would have to be established on a case-by-case basis.

There are limitations to the low-frequency sensitivity of spectral methods. Oscillations longer than 400 beats will not be resolved correctly with data segments of 400 beats. Fortunately much of the prognostic value in heart-rate variability seems to lie at frequencies much higher than this. Analysis over periods of 400 beats gives at least six times the minimum data length to detect oscillations of period 64 beats (Lotric *et al* 2000).

In our study, the patients with chronic heart failure were in a relatively mild and stable state (living at home) as distinct from the patients used by Ho *et al* (1997), who were acutely unwell and studied during an acute emergency admission to hospital.

5. Conclusions

We have shown, by considering the effect of the constituent operations of the DFA process upon a Taylor series expansion of the Fourier components of the signal, the equivalence between DFA and a new frequency-weighted form of power-spectral ratio. The α variable, calculated by DFA, of heart rate has recently been identified to have diagnostic and prognostic value in cardiovascular disease. Because of the steps involved in DFA, it has been described as a fractal measure, by implication different in nature from conventional spectral analyses. We can now see that α is intimately related to conventional spectral analysis and cannot any longer be considered to be in a different class of measurements. We have then experimentally verified a close correspondence between α as measured by DFA and an equivalent to α derived by frequency-weighted spectral analysis.

We can, therefore, now specify the differences between DFA and conventional spectral analysis:

1. The frequency ranges for DFA are fixed in cycles/beat whereas for conventional spectral analysis they are fixed in cycles s^{-1} (Hz). The relationship between these depends on heart rate.
2. α frequency-weights power spectra favour the centre frequency, de-emphasizing others in proportion to frequency-squared in both directions while conventional spectral analysis gives equal weight to all frequencies within its band of interest.

It now becomes clear why α_1 is low and α_2 sometimes high in patients with chronic heart failure, and why such abnormalities might in general predict poor prognosis. Heart failure is characterized by a decrease in the LF/HF ratio (an adverse prognostic marker) and therefore in the $2\Big/\left(1+\frac{\mathrm{HF}}{\mathrm{LF}}\right)$ ratio, so that α_1 (which is an indirect measure of the latter) is lower. Heart failure is also frequently associated with periodic breathing which can generate corresponding VLF rhythms in heart rate (Mortara *et al* 1997, Francis *et al* 2000). This, alone or in association with the reduced LF, may increase VLF/LF and thus the $2\Big/\left(1+\frac{\mathrm{LF}}{\mathrm{VLF}}\right)$ ratio and α_2.

Awareness of both the essential equivalence of (and the subtle distinctions between) DFA α and conventional spectral measures may now make it possible to identify which of these distinctions are responsible for the apparent improved prognostic power available in α.

References

Christini D J, Kulkari A, Sriker R, Stutman E R, Bennett F M, Haisdorff J M, Oriel N and Lutchen K R 1995 Influence of autoregressive model parameters on spectral estimates of heart rate dynamics *Ann. Biomed. Eng.* **23** 127–34

Eckberg D L 1997 Sympathovagal balance: a critical appraisal *Circulation* **96** 3224–32

Francis D P *et al* 2000 Very-low-frequency oscillations in heart rate and blood pressure in periodic breathing *Clin. Sci. (Colch)* **99** 125–32

Ho K K *et al* 1997 Predicting survival in heart failure case and control subjects by use of fully automated methods *Circulation* **96** 842–8

Huikuri H V *et al* 2000 Fractal correlation properties of R–R interval dynamics and mortality in patients with depressed left ventricular function after acute myocardial infarction *Circulation* **101** 47–53

Kaplan D T, Furman M I, Pincus S M, Ryan S M, Lipsitz L A and Goldberger A 1991 Aging and the complexity of cardiovascular dynamics *Biophys. J.* **59** 945–9

Kay S M and Marple S L 1981 Spectrum analysis—a modern perspective *Proc. IEEE* **69** 1380–419

La Rovere M T *et al* 1998 Baroreflex sensitivity and heart-rate variability in prediction of total cardiac mortality after myocardial infarction *Lancet* **351** 478–84

La Rovere M T *et al* 2001 Baroreflex sensitivity and heart rate variability in the identification of patients at risk for life-threatening arrhythmias *Circulation* **103** 2072–7

Lopera G A, Huikuri H V, Makikallio T H, Tapanainen J, Chakko S, Mitrani P D, Interian A, Castellanos A and Myerburg R J 2001 Is abnormal heart rate variability a specific feature of congestive heart failure? *Am. J. Cardiol.* **87** 1211–3

Lotric M B, Stefanovska A, Stajer D and Urbancic-Rovan V 2000 Spectral components of heart rate variability determined by wavelet analysis *Physiol. Meas.* **21** 441–57

Malliani A, Pagani M, Lombardi F and Cerutti C 1991 Cardiovascular neural regulation explored in the frequency domain *Circulation* **84** 484–92

Malpas S C 1998 The rhythmicity of sympathetic nerve acitivity *Prog. Neurobiol.* **56** 65–95

Mortara A *et al* 1997 Abnormal awake respiratory patterns are common in chronic heart failure *Circulation* **96** 246–52

Pagani M *et al* 1986 Power spectral analysis of heart rate and arterial pressure variabilities *Circ. Res.* **59** 178–93

Peng C K, Havlin S, Stanley H E and Goldberger A L 1995 Quantification of scaling exponents and crossover phenomena in nonstationary heartbeat time series *Chaos* **5** 82–7

Perkiomaki J S *et al* 2001 Comparability of nonlinear measures of HRV between long- and short-term electrocardiographic recordings *Am. J. Cardiol.* **87** 905–8

Pikkujamsa S M *et al* 1999 Cardiac interbeat interval dynamics from childhood to senescence *Circulation* **100** 393–9

Saermark K, Moeller M, Hintze U, Moelgaard H, Bloch T E, Huikuri H, Makkikiallio T, Levitan J and Lewkowicz M 2000 Comparison of recent methods of analysing heart rate variability *Fractals* **8** 315–22

Task Force of the European Society of Cardiology the North American Society of Pacing Electrophysiology 1996 Heart rate variability—standards of measurement, physiological interpretation and clinical use *Circulation* **93** 246–52

Tsuji H, Venditti F J Jr, Manders E S, Evans J C, Larson M G, Feldman C L and Levy D 1996 Determinants of heart rate variability *J. Am. Coll. Cardiol.* **28** 1539–46

Yeragani V K, Sobelewski E, Kay J, Jampala V C and Igel G 1997 Effect of age on long-term heart rate variability *Cardiovasc. Res.* **35** 35–42